

# Relationship between core temperature, skin temperature, and heat flux during exercise in heat

Xiaojiang Xu · Anthony J. Karis · Mark J. Buller · William R. Santee

Received: 26 February 2013 / Accepted: 30 May 2013 / Published online: 18 June 2013  
© Springer-Verlag Berlin Heidelberg (outside the USA) 2013

## Abstract

**Purpose** This paper investigates the relationship between core temperature ( $T_c$ ), skin temperature ( $T_s$ ) and heat flux (HF) during exercise in hot conditions.

**Method** Nine test volunteers, wearing an Army Combat Uniform and body armor, participated in three sessions at 25 °C/50 % relative humidity (RH); 35 °C/70 % RH; and 42 °C/20 % RH. Each session consisted of two 1-h treadmill walks at ~350 W and ~540 W intensity.  $T_s$  and HF from six sites on the forehead, sternum, pectoralis, left rib cage, left scapula, and left thigh, and  $T_c$  (i.e., core temperature pill used as a suppository) were measured. Multiple linear regressions were conducted to derive algorithms that estimate  $T_c$  from  $T_s$  and HF at each site. A simple model was developed to simulate influences of thermal conductivity and thickness of the local body tissues on the relationship between  $T_c$ ,  $T_s$ , and HF.

**Results** Coefficient of determination ( $R^2$ ) ranged from 0.30 to 0.88, varying with locations and conditions. Good sites for  $T_c$  measurement at surface were the sternum, and a combination of the sternum, scapula, and rib sites. The combination of  $T_s$  and HF measured at the sternum explained ~75 % or more of variance in observed  $T_c$  in hot environments. The forehead was found unsuitable for exercise in heat due to sweating and evaporative heat loss. The derived algorithms are likely applicable only for the

same ensemble or ensembles with similar thermal and vapor resistances.

**Conclusion** Algorithms for  $T_c$  measurement are location-specific and their accuracy is dependent, to a large degree, on sensor placement.

**Keywords** Non-invasive measurement · Heat strain · Human · Heat transfer

## Introduction

Heat illness and fatalities are a significant threat to military operations. There were 362 incident cases of heat stroke and 2,652 incident cases of other heat injury among US Armed Force active component members in 2011 (Armed Forces Health Surveillance Center 2012). The prevention of heat illness is especially challenging for critical occupations such as military, policemen, firefighters, and other emergency workers, as sometimes they must work at high intensity, often while wearing protective clothing and equipment, without regard to environmental conditions. The combination of high work intensity and protective clothing, which reduces the capacity for heat loss to the environment, significantly increases the potential for heat injury. Heat-related illnesses are also common in non-military populations, such as industrial workers (Donoghue 2004; Bonauto et al. 2007), sports (Howe and Boden 2007), and agricultural workers (Centers for Disease Control and Prevention 2008). There are various countermeasures and strategies to manage the heat injury. One of them is to use a physiological status monitoring (PSM) system to monitor the heat strain status (Bernard and Kenney 1994; Wan 2006; Tharion et al. 2010). The PSM system measures parameters such as heart rate, core temperature ( $T_c$ ), and

---

Communicated by George Havenith.

---

X. Xu (✉) · A. J. Karis · M. J. Buller · W. R. Santee  
Biophysics and Biomedical Modeling Division, US Army  
Research Institute of Environmental Medicine, 42 Kansas Street,  
Natick, MA 01760-5007, USA  
e-mail: xiaojiang.xu@us.army.mil

skin temperature ( $T_s$ ) so that early symptoms of heat illness can be detected and necessary interventions can be taken before the injury occurs.

Core temperature is an important indicator of heat strain status and is usually measured using rectal or esophageal probes or ingested telemetry pills. One PSM system (Equi-vital 1, Hidalgo Ltd. Cambridge, UK) uses telemetry temperature pills (Jonah<sup>TM</sup> Core Temperature Pill, Respironics, Bend, OR) to measure  $T_c$ . However, fluid ingestion can cause artifacts (Wikinson et al. 2008), and the use of disposable pills creates a logistical burden in the field, and even in clinical settings; thus, there have been on-going efforts to search for non-invasive approaches to measure  $T_c$  for about 40 years (Fox and Solman 1971; Yamakage and Namiki 2003; Dittmar et al. 2006; Gunga et al. 2008, 2009; Kimberger et al. 2009; Kitamura et al. 2010; Zeiner et al. 2010; Huang and Chen 2010; Teunissen et al. 2011; Steck et al. 2011). Many of these efforts are based on the zero heat flux (ZHF) principle proposed by Fox and Solman (1971). The ZHF system consists of a heat flux (HF) sensor, a heating disc, and a servo control system. The power to the heating disc is regulated to reach ZHF status, under which  $T_c$  is assumed to be equal to  $T_s$  measured by the HF sensor. Although ZHF systems have been widely used in cardiac surgery in Japan (Yamakage and Namiki 2003), they are not suitable for sustained field applications due to the power requirement. A “Double Sensor,” one type of HF sensor, has been developed to monitor heat strain of firefighters (Gunga et al. 2008). As several coefficients in their equations are not published, it is not possible to evaluate and use those equations. There also have been attempts to develop a surrogate  $T_c$  using the insulated skin temperatures for heat strain monitoring (Bernard and Kenney 1994; Taylor et al. 1998) and for monitoring circadian rhythm profiles (Gunga et al. 2009). A physiologically based Dynamic Bayesian Network model has been proposed to estimate internal temperature from the heart rate, accelerometry, and skin HF (Buller et al. 2011).

Despite these efforts, non-invasive estimation of  $T_c$  using HF sensors remains a challenge. The main reason is that the accuracy and reliability of estimating  $T_c$  from  $T_s$  and HF is inconsistent and can vary with the measurement location (Taylor and Amos 1997; Yamakage and Namiki 2003), clothing (Bernard and Kenney 1994; Taylor et al. 1998), and environmental conditions (Taylor et al. 1998; Gunga et al. 2008; Teunissen et al. 2011). There is a lack of understanding about the interaction among measurement location, properties of the body tissue, condition at skin surface, and clothing. In comparison with the clinical setting, monitoring  $T_c$  in the field is more difficult, as the human body and the environment are in dynamic rather than steady states. The purpose of the present study was to investigate the relationship between  $T_c$ ,  $T_s$ , and HF during exercise in heat through a human study and theoretical

analysis. Physiological data were used to determine which of the six locations used in the study were the most promising for non-invasive  $T_c$  measurement and to derive algorithms for  $T_c$  estimation from  $T_s$  and HF. A simple heat transfer model was developed to identify and analyze factors that affect the accuracy of  $T_c$  estimates, to gain insight into the mechanisms underlying  $T_c$  calculation based on measurements of HF sensors, and to guide algorithm development.

## Methods

### Subjects

Nine active duty military personnel from the Natick Soldier Center and Human Research Volunteer Program were enrolled as test volunteers after being informed of risks and purpose of the study, giving their written, informed consent, and being medically screened. The study was approved by the US Army Research Institute of Environmental Medicine’s Scientific and Human Use Review Committees. The volunteers were expressly assured that they were completely free to withdraw from participation in the study at any time. The characteristics (mean  $\pm$  SD) of the subjects were: age  $22 \pm 4$  years, height  $1.75 \pm 0.10$  m, weight  $76.4 \pm 10.7$  kg, and body fat  $23.4 \pm 5.8$  %. Percent body fat was determined by a Dual-Energy X-Ray Absorptiometry (Model: GE Lunar DXA, GE Healthcare, Waukesha, WI).

### Clothing ensembles

The subjects dressed in an ensemble consisting of the Army Combat Uniform (ACU), Interceptor Body Armor (BA) with front, back, and side ballistic inserts, ballistic collar, a Kevlar helmet, and running shoes. The thermal resistance and vapor resistance of the ensemble were  $0.24 \text{ m}^2 \text{ K W}^{-1}$  (1.56 clo) and  $34.99 \text{ m}^2 \text{ Pa W}^{-1}$ , measured at a wind speed of  $0.4 \text{ m s}^{-1}$ . The total weight of the body armor, including helmet, from size S to size XL, ranged from 13.03 to 16.64 kg.

### Experimental protocol

After arrival at the lab every morning, volunteers were encouraged to use the restroom, questioned regarding any health problems, and weighed wearing only undershorts. After instrumentation and dressing, volunteers rested in the dressing area for 30 min before entering the chambers. The test scenario began with 10 min standing rest, then a 60-min walk on the treadmill at a light-moderate metabolic rate of  $347 \pm 28 \text{ W}$  (mean  $\pm$  SD). The walk was followed

by a 30-min break. The volunteers entered the dressing area for weighing, and a restroom break, if needed. They then returned to sit in the chamber where they were provided drinking water, and seated to complete the break. Active testing then continued with another 10 min standing rest, a second 60-min walk on the treadmill at a moderate-heavy metabolic rate of  $536 \pm 32$  W, and a final 10-min standing rest. The safety limit for  $T_c$  was set at  $39.5$  °C. The volunteers could also withdraw from a test voluntarily, or be removed by test staff, at any time.

The volunteers participated in the three chamber test sessions. The three chamber conditions were warm [ $25$  °C,  $50$  % relative humidity (RH)], hot-humid ( $35$  °C,  $70$  % RH), and hot-dry ( $40$  °C,  $20$  % RH). Each session was separated by at least 4 days to minimize acclimation effects. Unless there was a make-up session, all chamber sessions followed the same order of presentation:  $25$  °C,  $50$  % RH;  $35$  °C,  $70$  % RH, and  $40$  °C,  $20$  % RH. Chamber air velocity (wind speed) was controlled at  $\sim 1.6$  m s<sup>-1</sup>. The Pandolf equation, which calculates the total metabolic rate according to body mass, external load, walking speed, and grade (Pandolf et al. 1977), was used to select combinations of treadmill speeds ( $0.9$ – $1.8$  m s<sup>-1</sup>) and slope ( $0$ – $5$  % grade) that approximated the targeted metabolic rates. In general, the metabolic target for the first walk could be reached by adjusting treadmill speed with no grade, whereas for the second walk, a slight grade was introduced to hold down the treadmill speed. A make-up session was scheduled if a volunteer was unable to complete a session as planned.

### Instrumentation

Core temperature was measured by a telemetry thermometer pill (Jonah<sup>TM</sup>, Core Temperature Pill, Respirationics, Bend, OR) used as a suppository to obtain a rectal temperature (O'Brien et al. 1998). The  $T_c$  signals were recorded by VitalSense<sup>®</sup> physiological monitor (Mini-mitter, Bend, OR). Five  $T_s$  and HF values were measured with ceramic heat flow sensors (FMS-060-TH44018-6, CE Concept Engineering, Old Saybrook, CT) on the surface of the forehead, sternum, left rib cage, left scapula, and left thigh. Data were recorded using a multi-channel data logger (Grant SQ2040-2F16, Grant Instruments, Hillsborough, NJ). A sixth HF sensor (see below) was placed over the left pectoralis major muscle. The locations for the placement of the HF sensors were selected on the basis of proximity to important anatomical features, and the ability to consistently place the sensors based on those anatomical landmarks and the results of previous studies (Taylor and Amos 1997; Yamakage and Namiki 2003). In addition, minimal interference to users and ease of placement were considered. All of the HF sensors were mounted on the skin

surface using an ECG foam adult monitoring electrode (40493E, Philips Electronics, Andover, MA). A hole, the diameter of the sensor, was cut in the center of the electrode. This created an adhesive ring of foam material that held the sensor in place, but allowed the top and bottom surfaces of the ceramic disc to be fully exposed. All the above measurements were recorded every 15 s. Heart rate and the sixth HF disc were measured and recorded by a PSM system (Equivital 1, Hidalgo Ltd., Cambridge, UK). Metabolic rate measurements were obtained by collecting expired air samples in Douglas bags for 2 min during rest periods immediately prior to exercise, and at approximately 20 min into each exercise period. The samples were then analyzed for oxygen uptake ( $\dot{V}O_2$ ) using a metabolic cart (True One 2400 Metabolic Measurement System, Parvo Medics Sandy, UT). The metabolic rates were measured to describe the intensity of exercise and to provide a measure of internal heat production.

### Statistical analysis

Multiple linear regression analysis was conducted to derive algorithms to predict the dependent variable  $T_c$  from two independent variables, the  $T_s$  and HF, at each site, using the data from all nine subjects (SigmaPlot for Windows version 11.0, Systat Software, Inc., San Jose, CA). The coefficient of determination ( $R^2$ ) is used to evaluate the association between  $T_c$ ,  $T_s$ , and HF at each site. As these two independent variables,  $T_s$  and HF, have different units, the regression coefficients do not necessarily represent their relative contribution to  $T_c$ . Thus, standardized regression coefficients were calculated to determine the contributions of each independent variable to predicting  $T_c$ . Furthermore, the relative contribution of each independent variable to  $R^2$  was estimated as follows (Havenith et al. 1998; DeGroot et al. 2006):  $\frac{\text{standardizedcoefficient}}{\sum \text{standardizedcoefficient}} \cdot R^2 \cdot 100$  %. The variance inflation factor (VIF) was also calculated to examine the presence of the collinearity among the independent variables. If VIF exceeded 4.0, collinearity among these variables became suspect (Fox 1991).

### Heat transfer analysis

The relationships between  $T_c$ ,  $T_s$ , and HF are complex and influenced by physical factors such as tissue thickness (e.g., skin, fat, bone) and tissue heat transfer characteristics (e.g., thermal conductivity, heat capacity). The relationships are also influenced by physiological factors, such as sweat evaporation and blood flow within the tissues. Figure 1a is a simplified physical heat transfer model of a single layer shell in a core–shell body ( $d$  is shell thickness), assuming that the heat transfer-related properties are uniform within

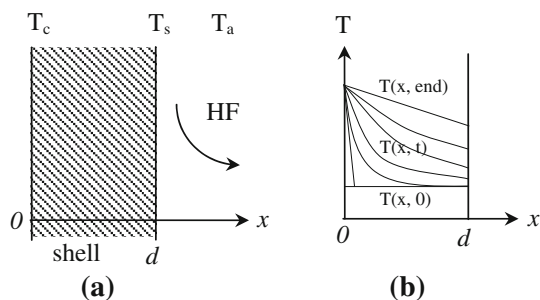


**Fig. 1** Schematic diagram of a shell layer in a core-shell body and heat transfer through the shell. **a** The heat transfers from the core-shell interface ( $T_c$ ) through the shell (thickness  $d$ ) to the skin surface ( $T_s$ ) by conduction, and from the skin surface to the external environment ( $T_a$ ) by convection, conduction, or radiation with total heat loss rate HF. **b** Dynamic temperature distribution at location  $x$  and time  $t$   $T(x, t)$  from initial steady state  $T(x, 0)$  to new steady state  $T(x, \text{end})$

the core. Metabolic heat is generated in the core and is transferred from the core ( $T_c$ ) through the tissue to the skin surface ( $T_s$ ) by conduction, then dissipates from the skin to ambient ( $T_a$ ) at a heat loss rate of HF by convection, evaporation, and radiation. The heat transfer process within the tissue is described by Eq. (1):

$$\rho c \frac{\partial T}{\partial t} = \lambda \frac{\partial}{\partial x} \left( \frac{\partial T}{\partial x} \right) \quad (1)$$

where  $T$  is the temperature ( $^{\circ}\text{C}$ ),  $t$  is time in second (s),  $x$  is the distance from the core to the tissue in meter (m),  $\rho$  is the density in  $\text{kg m}^{-3}$ ,  $c$  is the specific heat capacity in  $\text{J kg}^{-1} \text{ } ^{\circ}\text{C}^{-1}$ , and  $\lambda$  is the thermal conductivity in  $\text{W m}^{-1} \text{ } ^{\circ}\text{C}^{-1}$ . The following tissue parameters were used for the simulation:  $\rho$  is  $1,059 \text{ kg m}^{-3}$ ,  $c$  is  $3,899 \text{ J kg}^{-1} \text{ } ^{\circ}\text{C}^{-1}$ ,  $\lambda$  are  $0.20\text{--}0.70 \text{ W m}^{-1} \text{ } ^{\circ}\text{C}^{-1}$  (Werner and Buse 1988; Shitzer et al. 1996). The heat exchange at the inner surface (core surface) and the skin surface are defined by the boundary conditions, which differ between the steady state and transient conditions.

#### Steady state conditions

In the steady state, Eq. (1) can be theoretically solved, and the solution is:

$$T_c = T_s + \text{HF} \frac{d}{\lambda} \quad (2)$$

where  $d$  is the shell thickness in m. Equation (2) indicates that  $T_c$  can be calculated from  $T_s$  and HF when the  $d$  and  $\lambda$  of the tissue are known.

#### Transient conditions

The human body is rarely in a steady state condition; thus, the heat transfer process is often dynamic. Therefore, it is

important to determine whether Eq. (2) can be applied to transient conditions. Equation (1) can be numerically solved using the partial differential equation solver in MATLAB (Mathworks, Natick, MA). The solutions (i.e., transient temperature distributions over the tissue) reveal dynamic relationships between  $T_c$ ,  $T_s$ , and HF, thereby providing an indication of how Eq. (2) behaves under transient conditions.

Figure 1b is a schematic representation of the transient temperature distribution in the tissue from the initial steady state to a new steady state. Initially, the temperature over the tissue is a uniform temperature of  $33 \text{ } ^{\circ}\text{C}$ ; thus, the initial condition is  $T(x, 0) = 33 \text{ } ^{\circ}\text{C}$ . The transient process begins when  $T_c$  (i.e., the temperature at  $x = 0$ ) abruptly rises by  $1 \text{ } ^{\circ}\text{C}$  to  $34 \text{ } ^{\circ}\text{C}$ . Thus, the boundary condition at  $x = 0$  is  $T(0, t) = 34 \text{ } ^{\circ}\text{C}$  for  $t > 0$ . For simplicity, the following assumptions were made. The boundary condition at skin surface (i.e., at  $x = d$ ) is only convective heat loss. The convective heat transfer coefficient ( $\alpha$ ) is set at  $10 \text{ W m}^{-2} \text{ } ^{\circ}\text{C}$ , and the ambient temperature  $T_a$  is initially  $33 \text{ } ^{\circ}\text{C}$ . These initial and boundary conditions can be mathematically described by:

$$\begin{aligned} t = 0, T(x, 0) &= 33 \text{ } ^{\circ}\text{C} \\ t > 0, x = 0, T(0, t) &= 34 \text{ } ^{\circ}\text{C} \\ t > 0, x = d, -\lambda \frac{\partial T}{\partial x} &= \alpha(T(x, t) - T_a) \end{aligned} \quad (3)$$

The temperature distribution  $T(x, t)$  changes gradually until it reaches a new steady state [i.e.,  $T(x, \text{end})$ ]. During this transient period, the  $T_c$  value predicted by Eq. (2) will gradually converge on the true  $T_c$ . The response time is defined as the time required for the predicted  $T_c$  to reach the true  $T_c$ . It is the time lag between the predicted and true  $T_c$ , indicating how quick the predicted  $T_c$  traces the true  $T_c$ . A short response time is essential to high accuracy of predicted  $T_c$ . Thus, the response time is an indicator of whether Eq. (2) is applicable to transient conditions.

## Results

Typical results, including the observed  $T_c$ ,  $T_s$ , and HF of two sites, the forehead and sternum, at the  $40 \text{ } ^{\circ}\text{C}$  and  $20 \text{ } \%$  RH condition, are shown in Fig. 2. The term ‘‘observed  $T_c$ ’’ refers to the rectal temperature measured by the telemetry pill. After subjects moved from the preparation area to the chamber, at time  $-10 \text{ min}$ , due to the combined effect of increasing ambient temperature and physical activity,  $T_c$  and  $T_s$  began to rise. The HF initially dropped and stabilized before beginning to rise. Heat flux values fluctuated during the break period, as the subjects exited the chambers to be weighed, used the restroom if necessary, then

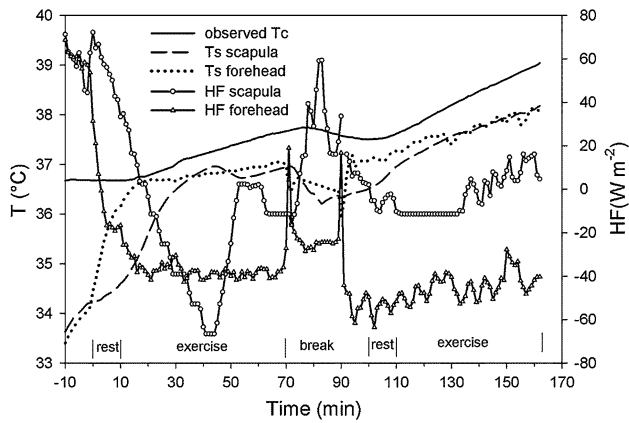


**Fig. 2** Representative results for the core temperature (observed  $T_c$ ), skin temperature ( $T_s$ ), and heat flux (HF) for the forehead and sternum at 40 °C and 20 % RH (hot-dry) conditions for various rest and exercise periods

re-entered, sat down, and were given water. Then, after being seated for approximately 20 min of the break period, they stood for the second 10 min standing baseline period.

Results of the multiple linear regression analysis for all conditions, including  $R^2$ , regression coefficients, and standardized coefficients, are summarized in Table 1. The dependent variable is observed  $T_c$  (°C), while independent variables are HF ( $W m^{-2}$ ) and  $T_s$  (°C). In addition to the six individual sites, Table 1 also includes the results for a regression based on the unweighted average of  $T_s$  and HF from the sternum, scapula, and rib (SSR), which yielded the highest  $R^2$  value, 0.79.

Table 2 showed  $R^2$  values for each separate condition and all conditions. Values of  $R^2$  for the sternum were the highest for combined results of all conditions, and were also the highest at 35 °C/70 % RH and 25 °C/50 % RH conditions. At 40 °C/20 % RH condition, the  $R^2$  value for the sternum was 0.75 and slightly lower than the  $R^2$  value for the rib of 0.77. Values of  $R^2$  for the forehead were consistently the lowest value. The  $R^2$  values for the unweighted average of three measurement sites (i.e., SSR) show slight improvements relative to the sternum. At 25 °C/50 % RH condition, most of the  $R^2$  values were below 0.51. All VIFs were less than 1.40, indicating no collinearity among the independent variables.

The results in Fig. 3 show the predicted response times versus representative values for tissue thickness and thermal conductivity. The thermal conductivities for the common “shell” tissues (i.e., bone, muscle, skin and fat) are about 0.75, 0.51, 0.47, and 0.21  $W m^{-1} °C^{-1}$ , respectively (Werner and Buse 1988). The response time represents how quickly the  $T_c$  estimated by Eq. (2) responds to a change in the  $T_c$ . Response times decrease as tissue thickness decreases and as tissue thermal conductivity increases. With a tissue thermal conductivity of

**Table 1** Multiple linear regression results

Location	$R^2$	Coefficients			Standardized coefficients*	
		Constant	HF	$T_s$	HF	$T_s$
Forehead	0.40	25.08	0.007	0.35	0.70 (18)	0.91 (23)
Sternum	0.75	20.08	0.015	0.48	0.42 (23)	0.92 (51)
Scapula	0.69	21.96	0.015	0.43	0.47 (24)	0.87 (45)
Pectoralis	0.60	23.76	0.003	0.40	0.21 (12)	0.81 (48)
Rib	0.70	26.51	0.018	0.31	0.66 (34)	0.70 (36)
Thigh	0.59	27.98	0.008	0.27	0.49 (24)	0.68 (34)
SSR	0.79	21.66	0.022	0.41	0.56 (31)	0.86 (48)

SSR combination of the sternum, scapula, and rib sites

\* Percentage of total variance explained by that independent variable in parentheses, the sum of the percentages of the total explained variance equals the  $R^2$

0.5  $W m^{-1} °C^{-1}$ , the response time is about 14 min for a tissue thickness of 1 cm, and the time increased to 45 min for a tissue thickness of 2 cm. With a tissue thickness of 1.5 cm, the response time was 19 min for a tissue with thermal conductivity of 0.7  $W m^{-1} °C^{-1}$  (e.g., bone), and rose to 55 min for a tissue with thermal conductivity of 0.2  $W m^{-1} °C^{-1}$  (e.g., fat).

**Discussion**

This study investigated factors that influence the relationship between  $T_c$ ,  $T_s$ , and HF in an attempt to develop a new, non-invasive method for monitoring heat strain during exercise in heat. The algorithms for  $T_c$  estimation at six locations of the human body (forehead, sternum, pectoralis, left rib cage, left scapula, and left thigh) were derived. A simple heat transfer model was developed and demonstrated influences of the body tissues and skin boundary conditions on the relationship between  $T_c$ ,  $T_s$ , and HF. The primary findings are (1) algorithms are location-specific and their accuracies vary with locations; (2) for the purpose of monitoring heat strain, a good location appears to be the sternum, and the forehead appears to be unsuitable; and (3)  $T_s$  and HF measured at the sternum explains ~75 % or more of variance in observed  $T_c$  in hot conditions.

Placement of the HF sensor is critical to the accuracy of  $T_c$  measurement. Values of  $R^2$  vary with locations, as shown in Tables 1 and 2. For instance,  $R^2$  values change from 0.85 at the sternum to 0.47 on the forehead at 35 °C/70 % RH condition. Even though the forehead is the most common location in a clinical setting where patients are usually at rest (Yamakage and Namiki 2003; Dittmar et al. 2006; Gunga et al. 2008; Kimberger et al. 2009; Kitamura et al. 2010; Zeiner et al. 2010; Teunissen et al.



**Table 2** Coefficient of determination ( $R^2$ ) for each condition and all conditions

	Forehead	Sternum	Scapula	Pectoralis	Rib	Thigh	SSR
40 °C/20 % RH	0.47	0.75	0.72	0.73	0.77	0.61	0.81
35 °C/70 % RH	0.47	0.85	0.82	0.67	0.82	0.71	0.88
25 °C/50 % RH	0.30	0.51	0.42	0.40	0.37	0.39	0.49
All	0.40	0.75	0.69	0.60	0.70	0.59	0.79

SSR combination of the sternum, scapula, and rib sites

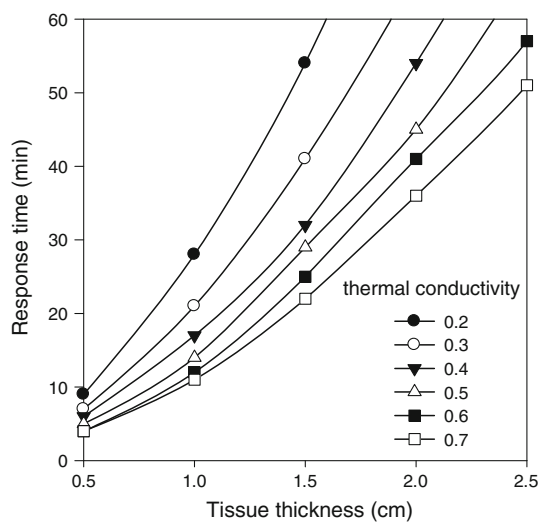


**Fig. 3** Theoretical response times as a function of the tissue thickness, with various tissue thermal conductivities ranging from 0.2 to 0.7  $\text{W m}^{-1} \text{°C}^{-1}$

2011), the results of this study demonstrated that the forehead is not suitable for monitoring heat strain during exercise. The sensor adhering on the forehead often becomes loose due to heavy sweating; thus, the measurement is less reliable during intense exercise or heat exposure. In addition, elevated evaporative heat loss on the forehead may cause errors in  $T_c$  estimation (see analysis below). This indicates that the level of physical activity (i.e., anticipated sweat level) or application (i.e., rest or exercise) should be taken into account when selecting a sensor location. Of the six sites studied, the results in Tables 1 and 2 indicated that most favorable locations were on the upper torso, with the best location on the sternum.

In addition to the context of the activity, the algorithms are also location-specific. Equation (2) includes a term  $d/\lambda$ , which represents properties of local tissues and indicates that the location impacts the relationship between  $T_c$ ,  $T_s$ , and HF. As shown in Table 1, equations for each location have different constants and coefficients. In a similar manner, for the Double Sensor systems, different equations were used, depending on whether the sensor was placed inside a helmet (Gunga et al. 2008), or on the forehead (Kimberger et al. 2009). Practical interpretation of this

finding is that a non-invasive method using the HF sensor should be used only in the location for which the method was developed to avoid introducing additional errors.

The heat transfer model developed in this study demonstrated the impacts of tissue properties on the accuracy of  $T_c$  measurements. Figure 3 indicates that a good location for  $T_c$  measurement should have high tissue thermal conductivity and thin tissue thickness (i.e., the distance from the core to the surface). The forehead is theoretically a good location, as it is close to the brain and the main “shell” tissue is bone that has heat conductivity among the highest of all body tissues. The sternum is a good location, as it is close to the heart and pulmonary blood vessels, which are possibly the most representative sites for body core temperature. The sternum tissues are mainly bone, cartilage, and skin. Fat tissues, which have the lowest thermal conductivity of the body tissues, are minimal in these areas. An early study recommended that the forehead, occipital region, and upper sternum were considered good locations for  $T_c$  measurement in clinical settings (Yamakage and Namiki 2003). Two theoretical studies also showed that accuracy of  $T_c$  measurement on skin surface is influenced by the local tissue thickness (Kitamura et al. 2010; Steck et al. 2011). Results of the heat transfer simulation supported our finding from the human study that the sternum is a promising location for non-invasive  $T_c$  measurement during exercise in heat.

The heat transfer model also reveals the potential impact of boundary conditions near the sensor on  $T_c$  measurement (i.e., the effects of evaporation and clothing). As shown in Fig. 1, the HF is the total heat loss at skin surface and includes convection/radiation ( $\text{HF}_d$ ) and evaporation ( $\text{HF}_e$ ). In other words, the HF in Eq. (2) is supposed to be total HF which equals to  $\text{HF}_d + \text{HF}_e$ . However, an HF sensor measures the heat loss (i.e., the heat flux) using only the temperature difference (i.e., sensible heat loss). The sensor does not capture the evaporative heat transfer driven by the vapor pressure gradient (i.e., insensible heat loss). Thus, an HF sensor measures only sensible heat loss (i.e.,  $\text{HF}_d$ ), and neglects evaporative heat loss (i.e.,  $\text{HF}_e$ ). Therefore, the HF measured by an HF sensor is actually less than the HF in Eq. (2), which is the total HF. Thus,  $\text{HF}_e$  is neglected in the measurement and calculation, and could potentially

contribute to the error in  $T_c$  measurement. The error caused by evaporation may be high when an HF sensor is placed on open skin area, such as the forehead, where evaporation is high. The forehead is considered to be a region with high sweat production (Machado-Moreira et al. 2007). Therefore, the evaporation of sweat is another reason that the accuracy of  $T_c$  measurement at the forehead was low in our study.

To reduce the influence of sweat evaporation, the HF sensor should be placed in a location where evaporative heat loss is minimal. In this study, the sensors on the torso were covered by body armor, and in a previous study the Double Sensor was covered by the helmet (Gunga et al. 2008). The low permeability of the body armor and helmet reduces evaporative heat loss in the covered area and, thus, likely reduces the error and increases the accuracy of  $T_c$  measurement. Previous studies showed that relationship between estimated  $T_c$  and observed  $T_c$  are dependent on the ensemble worn over the sensors (Bernard and Kenney 1994). Therefore, it is likely that algorithms derived in the study will be applicable only to the ensembles used in this study or ensembles with similar thermal and vapor resistances.

The algorithms are influenced by the environment to a certain degree, as shown in Table 2. At the low stressful temperature of 25 °C,  $R^2$  values were low, and the highest was  $R^2$  of 0.51 at the sternum. However, at hot environments of 35 °C or 40 °C, the sternum  $R^2$  increased to 0.85 or 0.75, respectively. This indicated that the combination of  $T_s$  and HF explained ~75 % or more of variance in observed  $T_c$  in hot environments. Our main focus was to find non-invasive approaches to monitor heat strain, which generally is more likely to occur in hot environments. For those stressful conditions, an  $R^2$  of this magnitude suggests that it is promising to use  $T_s$  and HF measured at the sternum to monitor heat strain.

The algorithms developed in this study are simple and use only  $T_s$  and HF measured using an HF sensor. Linear equations using those two variables were chosen to estimate  $T_c$ , because they were consistent with the result of heat transfer analysis [i.e., Eq. (2)]. The simple computation does not require any additional inputs or measurements. The Double Sensor is, in principle, an HF sensor, but the  $T_c$  calculation algorithm requires inputs for the thermal conductivities of human tissues and the heat transfer coefficient from the skin surface to the ambient air (10–30 W m<sup>-2</sup> K<sup>-1</sup>) (Gunga et al. 2008). The dual-heat-flux sensor requires the derivation of a thermal resistance ratio, which is influenced by environmental conditions, to calculate  $T_c$  (Kitamura et al. 2010). The ZHF-based system requires those extra components plus a power supply, which results in a more complicated system than an HF-based system.

The preceding analysis indicates that a non-invasive measurement of  $T_c$  based on skin surface measurements may be influenced by multiple factors such as measurement site, evaporation, and clothing. It is worth exploring options that could attenuate these influences to improve the methodology. One option would be to use three sensors at three locations such as sternum, scapula, and rib. The results in Tables 1 and 2 show the improvement provided using three sensors versus one sensor. For field applications, this would increase reliability, as  $T_c$  could still be obtained, even if only one sensor is functional. Another option would be to use the recently developed dual-heat-flux sensor (Kitamura et al. 2010). It consists of two materials with two thicknesses, and actually measures two heat fluxes and four temperatures. In theory, the dual-heat-flux sensor does not require parameters of body tissues for  $T_c$  measurement. This type of sensor could potentially reduce the influence of local tissue properties on  $T_c$  measurement, thus improving accuracy.

A limitation of this study is that the experiments were conducted only in one ensemble. As analyzed in the analysis, the clothing impacted the relation among  $T_c$ ,  $T_s$ , and HF. Therefore, the algorithms developed in this study are likely to be applicable only for monitoring heat strain in military or police training, or tactical operations where the ensembles worn had the same or similar thermal properties to the one in this study (i.e., a standard uniform and body armor). Further studies are needed to determine how clothing affects these algorithms and to develop an ensemble correction factor to make these algorithms applicable to a series of ensembles. It will also be necessary to conduct human studies or field studies to determine if these algorithms are suitable for a wider range of conditions or operational settings. Another limitation is that the results were compared mainly with results collected in clinical settings which might not be comparable to soldiers in the field. Most published studies focus on clinical applications. One study did focus on field application for fighters (Gunga et al. 2008), but the sensor location differed from the present study, and the equation coefficients were not published. Therefore, it was not possible to use these data for comparison purposes.

## Conclusion

The relationship between  $T_c$ ,  $T_s$ , and HF was analyzed by applying heat transfer analysis to human experimental data. Algorithms were derived to estimate  $T_c$  from  $T_s$  and HF measured at forehead, sternum, pectoralis, left rib cage, left scapula, and left thigh. The heat transfer simulation demonstrated the influences of local body tissue properties (i.e., thermal conductivity and thickness) on the relationships

between  $T_c$ ,  $T_s$ , and HF. Algorithms for  $T_c$  measurement are location-specific and their accuracy is dependent, to a large degree, on sensor placement. For the sites studied, the best locations appeared to be the sternum, or a combination of the sternum, scapula and rib sites. The combination of  $T_s$  and HF measured at the sternum explained  $\sim 75\%$  or more of variance in observed  $T_c$  in hot environments. The forehead, which is the most common location for non-invasive  $T_c$  measurements in a clinical setting, was found to be unsuitable for use during exercise in the heat due to sweating and evaporative heat loss. The derived algorithms are likely applicable only for the same ensemble or ensembles with similar thermal and vapor resistances.

**Acknowledgments** We would like thank to the volunteers who endured the experimental heat trials. We would also like to thank Dr. Reed Hoyt for his critical review and comments of this manuscript. We would like to acknowledge and thank Mr. Stephen Mullen, Patel Tejash, Timothy Rioux, Julio Gonzalez, William Tharion, Alex Welles, and Ms. Laurie Blanchard for their technical assistance in the collection, organization, and analysis of the study data.

**Disclaimer** This study is approved for public release; distribution is unlimited. The opinions or assertions contained herein are the private views of the author(s) and are not to be construed as official or reflecting the views of the Army or the Department of Defense. The investigators have adhered to the policies for protection of human subjects as prescribed in Army Regulation 70-25, and the research was conducted in adherence with the provisions of 32 CFR Part 219. Human subjects participated in these studies after giving their free and informed voluntary consent. Investigators adhered to AR 70-25 and USAMRMC Regulation 70-25 on the use of volunteers in research. Any citations of commercial organizations and trade names in this report do not constitute an official Department of the Army endorsement of approval of the products or services of these organizations.

## References

- Armed Forces Health Surveillance Center (2012) Heat injuries, active component, U.S. Armed Force, 2011. *MSMR* 19:14–16
- Bernard TE, Kenney WL (1994) Rationale for a personal monitor for heat strain. *Am Ind Hyg Assoc J* 55:505–514
- Bonauto DB, Anderson R, Rauser E, Burke B (2007) Occupational heat illness in Washington State, 1995–2005. *Am J Ind Med* 50:940–950
- Buller MJ, Castellani J, Robert WS, Hoyt RW, Jenkins OC (2011) Human thermoregulatory system state estimation using non-invasive physiological sensors. *Conf Proc IEEE Eng Med Biol Soc* 2011:3290–3293
- Centers for Disease Control and Prevention (2008) Heat-related deaths among crop workers—United States, 1992–2006. *MMWR Morb Mortal Wkly Rep* 57:649–653
- DeGroot DW, Havenith G, Kenney WL (2006) Responses to mild cold stress are predicted by different individual characteristics in young and older subjects. *J Appl Physiol* 101:1607–1615
- Dittmar A, Gehin C, Delhomme G, Boivin D, Dumont G, Mott C (2006) A non-invasive wearable sensor for the measurement of brain temperature. *Engineering in Medicine and Biology Society, 2006 EMBS 06, 28th Annual International Conference of the IEEE*, 900–902
- Donoghue AM (2004) Heat illness in the U.S. mining industry. *Am J Ind Med* 45:351–356
- Fox J (1991) *Regression diagnostics: an introduction*. Sage, Newbury Park
- Fox RH, Solman AJ (1971) A new technique for monitoring the deep body temperature in man from the intact skin surface. *J Physiol* 212:8–10
- Gunga HC, Sandsund M, Reinertsen RE, Sattler F, Koch J (2008) A non-invasive device to continuously determine heat strain in humans. *J Therm Biol* 33:297–307
- Gunga HC, Werner A, Stahn A, Steich M, Schlabs T, Koralewski E, Kunz D, Belavy DL, Felsenberg D, Sattler F, Koch J (2009) The Double Sensor—a non-invasive device to continuously monitor core temperature in humans on earth and in space. *Respir Physiol Neurobiol* 169:S63–S68
- Havenith G, Coenen J, Kistemaker L, Kenney WL (1998) The relevance of individual characteristics for human heat stress response is dependent on work intensity and climate type. *Eur J Appl Physiol* 77:231–241
- Howe AS, Boden BP (2007) Heat-related illness in athletes. *Am J Sports Med* 35:1384–1395
- Huang M, Chen W (2010) Theoretical simulation of the dual-heat-flux method in deep body temperature measurements. In: 32nd Annual International Conference of the IEEE EBS, 561–564
- Kimberger O, Theil R, Schuh M, Koch J, Sessler DL, Kurz A (2009) Accuracy and precision of a novel non-invasive core thermometer. *Br J Anaesth* 103:226–231
- Kitamura KI, Zhu X, Chen W, Nemoto T (2010) Development of a new method for the noninvasive measurement of deep body temperature without a heater. *Med Eng Phys* 32:1–6
- Machado-Moreira CA, Wilmsink F, Meijer A, Mekjavic IB, Taylor NAS (2007) Chrome domes: sweat secretion from the head during thermal strain. In: Mekjavic IB, Kounalakis SN, Taylor NAS (eds) *Proceedings of 12th International Conference on Environmental Ergonomics*. Piran, Slovenia, pp. 272–274
- O'Brien C, Hoyt RW, Buller MJ, Castellani JW, Young AJ (1998) Telemetry pill measurement of core temperature in humans during active heating and cooling. *Med Sci Sports Exerc* 30(3):468–472
- Pandolf K, Givoni B, Goldman RF (1977) Predicting energy expenditure with loads while standing or walking very slowly. *J Appl Physiol Respir Environ Exerc Physiol* 43:577–581
- Shitzer A, Stroschein LA, Gonzalez RR, Pandolf K (1996) Lumped-parameter tissue temperature-blood perfusion model of a cold-stress fingertip. *J Appl Physiol* 80:1829–1834
- Steck LN, Sparrow EM, Abraham JP (2011) A non-invasive measurement of the human core temperature. *Int J Heat Mass Transf* 54:975–982
- Taylor NAS, Amos D (1997) Insulated skin temperature and cardiac frequency as indices of thermal strain during work in hot environments. Technical Report DSTO-TR-0590, Defense Science and Technology Organization, Australia
- Taylor NAS, Wilmsmore BR, Amos D, Takken T, Komen T, Cotter JD, Jenkins A (1998) Indirect measurement of core temperature during work: clothing and environment influences. In: Hodgdon JA, Heaney JH, Buono MJ (eds) *Environmental Ergonomics VIII*. Naval Health Research Center and San Diego State University, San Diego
- Teunissen LPJ, Klewer J, Sterz F, Haan AD, Koning JJD, Daanen HAM (2011) A non-invasive continuous temperature measurement by zero heat flux. *Physiol Meas* 32:559–570
- Tharion WJ, Buller MJ, Karis AJ, Hoyt RW (2010) Development of a remote medical monitoring system to meet soldier needs. In: Karowski W, Salvendy G (eds), *Proceedings of the 3rd*



- International Conference on Applied Human Factors and Ergonomics. USA Publishing, Louisville
- Wan M (2006) Assessment of occupational heat strain. PhD Thesis, University of South Florida
- Werner J, Buse M (1988) Temperature profiles with respect to inhomogeneity and geometry of the human body. *J Appl Physiol* 65:1110–1118
- Wikinson DM, Carter JM, Richmond VL, Backer SD, Rayson MP (2008) The effect of cool water ingestion on gastrointestinal pill temperature. *Med Sci Sports Exerc* 40:523–528
- Yamakage M, Namiki A (2003) Deep temperature monitoring using a zero-heat-flow method. *J Anesth* 17:108–115
- Zeiner A, Klewer J, Sterz F, Haugk M, Krizanac D, Testori C, Losert H, Ayati S, Holzer M (2010) A non-invasive continuous cerebral temperature monitoring in patients treated with mild therapeutic hypothermia: an observation pilot study. *Resuscitation* 81:861–866